ELEMENTA
Science of the Anthropocene

Roukaerts, A, et al. 2021. The biogeochemical role of a microbial biofilm in sea ice: Antarctic landfast sea ice as a case study. *Elem Sci Anth*, 9: 1. DOI: https://doi.org/10.1525/elementa.2020.00134

RESEARCH ARTICLE

The biogeochemical role of a microbial biofilm in sea ice: Antarctic landfast sea ice as a case study

Arnout Roukaerts[1], Florian Deman[1,2], Fanny Van der Linden[2,3], Gauthier Carnat[3], Arne Bratkic[1,2], Sebastien Moreau[4], Delphine Lannuzel[5], Frank Dehairs[1], Bruno Delille[2], Jean-Louis Tison[3], and François Fripiat[3,*]

A paradox is commonly observed in productive sea ice in which an accumulation in the macro-nutrients nitrate and phosphate coincides with an accumulation of autotrophic biomass. This paradox requires a new conceptual understanding of the biogeochemical processes operating in sea ice. In this study, we investigate this paradox using three time series in Antarctic landfast sea ice, in which massive algal blooms are reported (with particulate organic carbon concentrations up to 2,600 μmol L^{-1}) and bulk nutrient concentrations exceed seawater values up to 3 times for nitrate and up to 19 times for phosphate. High-resolution sampling of the bottom 10 cm of the cores shows that high biomass concentrations coexist with high concentrations of nutrients at the subcentimeter scale. Applying a nutrient-phytoplankton-zooplankton-detritus model approach to this sea-ice system, we propose the presence of a microbial biofilm as a working hypothesis to resolve this paradox. By creating microenvironments with distinct biogeochemical dynamics, as well as favoring nutrient adsorption onto embedded decaying organic matter, a biofilm allows the accumulation of remineralization products (nutrients) in proximity to the sympagic (ice-associated) community. In addition to modifying the intrinsic physicochemical properties of the sea ice and providing a substrate for sympagic community attachment, the biofilm is suggested to play a key role in the flux of matter and energy in this environment.

Keywords: Biogeochemistry, Sea ice, Nutrient cycling, Microbial biofilm

1. Introduction

Sea ice plays a significant role in biogeochemical cycles, providing an active biogeochemical interface at the ocean-atmosphere boundary (Vancoppenolle et al., 2013). Permeated by a network of channels, pores, and intracrystalline inclusions, sea ice and its brine-filled spaces are colonized by a sympagic (ice-associated) community that is both taxonomically diverse and metabolically active (Thomas and Dieckmann, 2002). This sympagic community is thought to play a significant role in structuring the biogeochemical dynamics and food webs of polar oceans (e.g., Lannuzel et al., 2020, and references therein). Sympagic microbial adaptations involve changes in intracellular processes, but also in extracellular controls. In particular, microbially secreted extracellular polymeric substances (EPS) have been shown to modify the functioning of the microbial community and the physicochemical properties of the ice, including on the microscale (Krembs et al., 2002; Krembs et al., 2011; Meiners et al., 2003; Meiners et al., 2004; Meiners et al., 2008; Krembs and Deming, 2008; Underwood et al., 2010; Ewert and Deming, 2013). Bacterial communities in sea ice also appear to be much more productive than their pelagic counterparts and taxonomically and functionally distinct from them (Kaartokallio et al., 2013; Bowman, 2015). Traditionally, sea-ice biogeochemical studies have been based on methods and concepts inherited from planktonic research. However, in terms of organism distribution, fluid (and nutrients) transport, and predator–prey interactions, a seawater model is perhaps less useful for conceptualizing the sympagic community than models developed for porous substrates such as soils or sediments (Krembs et al., 2000).

Our present-day understanding of nutrient dynamics in sea ice is suffering from this interpretation bias. Nutrients are considered to behave like major dissolved sea salts: homogeneously distributed across the brine network (conservative with salinity), transported with brine motion,

[1] Analytical, Environmental, and Geochemistry, Earth Sciences Research Group, Vrije Universiteit Brussel, Brussels, Belgium
[2] Unité d'océanographie chimique, Freshwater and Oceanic Science Unit of Research (FOCUS), Université de Liège, Liège, Belgium
[3] Laboratoire de Glaciologie, Department of Geosciences, Environment and Society, Université libre de Bruxelles, Brussels, Belgium
[4] Norwegian Polar Institute, Tromsø, Norway
[5] Institute for Marine and Antarctic Studies, University of Tasmania, Hobart, Tasmania, Australia
* Corresponding author:
Email: francois.fripiat@ulb.be

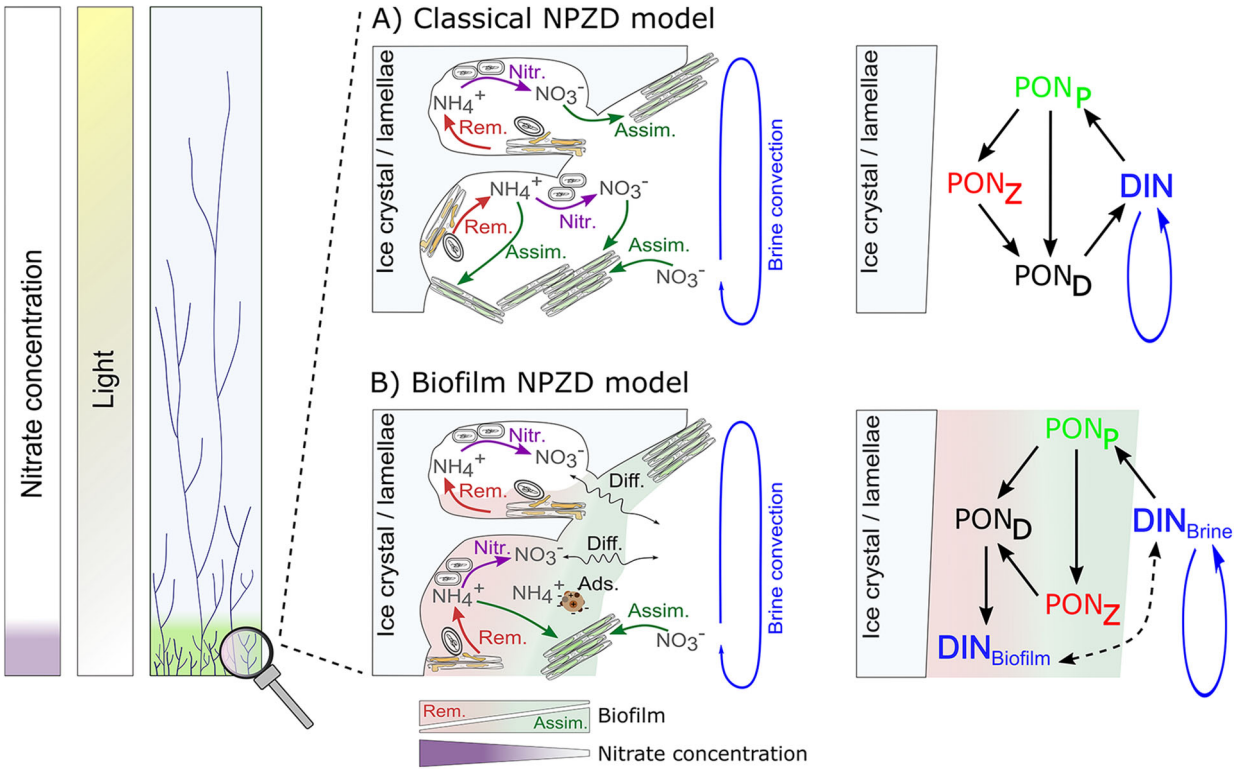

Figure 1. Representation of nitrogen dynamics in sea ice under the current paradigm and biofilm-included nutrient-phytoplankton-zooplankton-detritus (NPZD) model. The current paradigm (A) of nutrient dynamics in the brine network, with inorganic nutrients (represented by inorganic nitrogen) located in the brine network where nitrate can be assimilated (Assim.), particulate organic nitrogen (PON) can be remineralized (Rem.) and ammonium can be assimilated or nitrified (Nitr.). The schematic NPZD model on the right has four different nitrogen pools: dissolved inorganic nitrogen (DIN, where DIN = $NO_3^- + NO_2^- + NH_4^+$; nutrient pool in the model), PON_P = phytoplankton, PON_Z = zooplankton, and PON_D = detritus. Arrows represent the fluxes between the different pools (e.g., growth, grazing, mortality). The model includes DIN exchange with the underlying seawater through brine movement and/or diffusion. The new paradigm (B) includes a biofilm that allows for gradients between autotroph-dominated (assimilating) and heterotroph-dominated (remineralizing) communities, as well as nutrient adsorption (Ads.) on EPS and decaying organic matter. Remineralization and nitrification can also take place in brine pockets that are isolated due to clogging of the brine network by the biofilm. In the schematic biofilm-NPZD model, the nutrient pool is split into DIN in brine (DIN_{brine}) and DIN in biofilm ($DIN_{biofilm}$). Zigzag arrows are for diffusion between the biofilm and the surrounding brines. Brine convection represents mixing between brines and the underlying seawater (e.g., brine convection, brine pumping, other interface processes). Color gradients in fillings suggest relative intensity/concentration. DOI: https://doi.org/10.1525/elementa.2020.00134.f1

and exchanged with seawater in permeable sea ice (**Figure 1A**). In addition, their dynamic is thought to be driven by microbially mediated consumption and assimilation into biomass and by production sustained by nutrient supply from remineralization (Fripiat et al., 2017). Most of the sea-ice biogeochemical models are in line with this paradigm (Vancoppenolle and Tedesco, 2017), with the simple expression being represented by the NPZD model in **Figure 1A** (with N for nutrients, P for phytoplankton, Z for zooplankton, and D for detritus). However, this paradigm cannot satisfactorily explain many observations in productive sea ice (Arrigo et al., 1995; Riaux-Gobin et al., 2005; Cozzi, 2008; Becquevort et al., 2009; Riaux-Gobin et al., 2013; Lannuzel et al., 2014; Miller et al., 2015; Fripiat et al., 2017), in which high biomass concentrations often coexist with very high concentrations of inorganic nutrients (hereafter referred to as the "sea-ice nutrient paradox").

In this study, we examine data obtained from three time series in Antarctic landfast sea ice and discuss the presence of a microbial biofilm in sea ice as a working hypothesis for the sea-ice nutrient paradox (**Figure 1B**). We follow the International Union of Pure & Applied Chemistry terminology for biofilm (Vert et al., 2012; Flemming et al., 2016), defined as an aggregate of microorganisms in which cells that are frequently embedded within a self-produced matrix of EPS adhere to each other and/or to a surface. The proposed sea-ice biofilm maintains decaying products in proximity to the sympagic community and favors nutrient adsorption onto decaying organic matter. As already suggested by Krembs and Deming (2008), it also creates chemical gradients which in turn allow the formation of

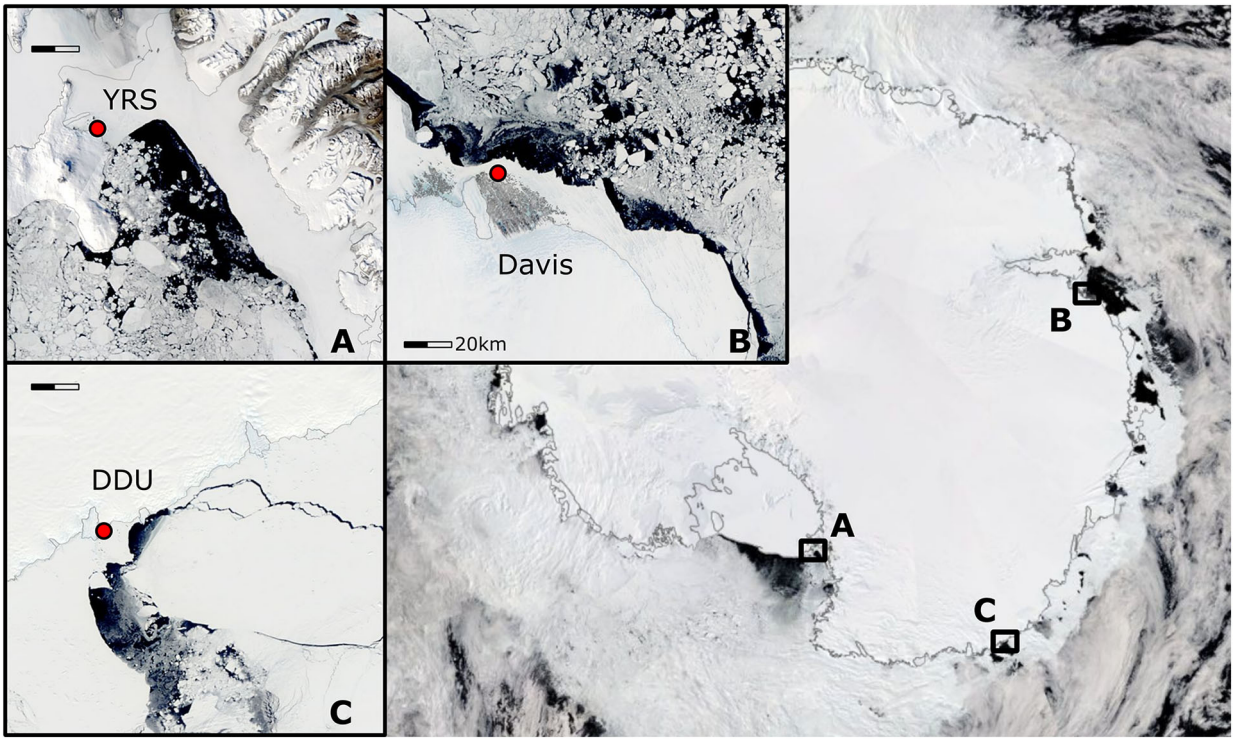

Figure 2. Location of the three sampling sites of Antarctic landfast sea ice. (A). YROSIAE station (2011–2012), Cape Evans, McMurdo Sound, Ross Sea. (B) Davis Station (2015), Abatus Bay, Prydz Bay. (C) DDU station (2011) near Dumont d'Urville, Terre Adélie. We acknowledge the use of imagery from the NASA Worldwide application (https://worldview.earthdata.nasa.gov), part of the NASA Earth Observing System Data and Information System (EOSDIS): November 29, 2012, for YROSIAE, November 2, 2015, for DAVIS, and October 18, 2011, for DDU. DOI: https://doi.org/10.1525/elementa.2020.00134.f2

contrasted biogeochemical environments at the microscale. The biofilm is therefore suggested to play a key role in nutrient mobility and availability in productive sea-ice environments.

2. Material and methods

2.1. Location of the study sites

New data sets sampled during the Year Round survey of Ocean-Sea Ice-Atmosphere Exchanges (YROSIAE) campaign at Cape Evans and a field campaign at Davis Station were combined with published data (Fripiat et al., 2015) from a time series in the vicinity of Dumont d'Urville (hereafter referred to as DDU; **Figure 2**). The YROSIAE sampling was carried out nearby the New Zealand permanent Antarctic research station Scott Base, located in McMurdo Sound (Ross Sea). The field campaign consisted of a first leg (November 28 to December 8, 2011, hereafter referred to as YROSIAE-1) and continued during the next spring for the second leg (September 19 to November 30, 2012, hereafter referred to as YROSIAE-2). Ice cores and underlying seawater were collected on 12 occasions about 1 km off Cape Evans (77° 38′ S, 166° 23′ E). Sampling was also carried out at Abatus Bay (68° 34′ 36″ S, 77° 58′ 03″ E), approximately 2 km north of the Australian research station Davis Station, located in Prydz Bay. Ice cores and underlying seawater were sampled on six occasions in spring between October 27 and December 11, 2015. Sampling at Dumont d'Urville was carried out close to the French research station at Terre Adélie, west of the Géologie Archipelago (66° 39′ 55″ S, 139° 59′ 32″ E) from June 30 to November 24, 2011. Ice cores and underlying seawater were collected on nine occasions. Sampling at DDU was done for particulate organic nitrogen (PON), dissolved organic nitrogen (DON), and dissolved inorganic nitrogen (i.e., the sum of nitrate, NO_3^-, nitrite, NO_2^-, and ammonium, NH_4^+). Full details on sampling and sample processing at DDU can be found in Fripiat et al. (2015).

2.2. Field sampling procedure

Ice cores were collected at regular time intervals in a selected area of approximately 10 × 10 m for each sampling occasion, adjacent to the site of the preceding sampling. These sampling zones were kept close to each other to minimize the potential for spatial variability. Although the ice was of uniform consolidation, we acknowledge that a time series such as conducted here may be affected by spatial variability, the impact of which could not be fully assessed when discussing the temporal evolution of the biogeochemical processes. Accordingly, only large variations of biomass and nutrients are discussed, such as the one associated with the growth and decay of the bottom sea-ice algal bloom.

Cores were collected using an electropolished stainless-steel ice corer (14 cm internal diameter; hereafter referred

as ID) for YROSIAE and DDU, and a KOVACS corer (14 cm ID, Roseburg, OR, USA) for Davis. In situ ice temperature was measured directly on one dedicated core at 5-cm intervals along the core using a temperature probe (TESTO®720, Lenzkirch, Germany). Ice textures were determined on thin sections (600–700 μm) installed on a light table equipped with cross-polarized sheets. Textural types were identified based on visual observation of the size, shape, and orientation of the ice crystals according to the literature (Eicken et al., 1991; Tison et al., 1998).

For YROSIAE, a core for salinity and biogeochemical parameters (nutrients and biomass) was collected, stored directly horizontally at −20 °C to avoid brine drainage, and processed the same day in the shore-based laboratory. The cores were cut lengthwise, with one half used for determining NO_3^-, NO_2^-, NH_4^+, phosphate (PO_4^{3-}), particulate organic carbon (POC), and PON concentrations, and the other half for silicic acid ($Si(OH)_4$), biogenic silica ($bSiO_2$), and lithogenic silica (LSi) concentrations. For each core, five ice slices (of 10-cm length at the ice-core bottom but >10 cm higher up in the core, depending on the ice thickness) were cut with a band saw and melted the same day at room temperature in the dark. The samples were filtered immediately through precombusted GF/F filters (0.7 μm porosity; Whatman, Little Chalfont, United Kingdom) or polycarbonate membranes (0.4 μm porosity; Nuclepore Agar Scientific, Stansted, United Kingdom), with the latter only for $bSiO_2$ and LSi analysis. The GF/F filters were stored at −20 °C for POC and PON measurements. The polycarbonate membranes were dried overnight at 50 °C and stored in the dark at ambient temperature. The filtrate was stored either in 60-ml acid-washed, prerinsed polyethylene bottles at −20 °C for nutrients or in 60- to 250-ml acid-washed, prerinsed polypropylene bottles at ambient temperature in the dark for $Si(OH)_4$. For each sample, a subsample was taken for salinity measurements (Thermo Fisher Scientific Inc. WP-84TP, Waltham, MA, USA). The bottom ice sections during YROSIAE were melted sequentially at ambient temperature in the dark (four sequential fractions per ice block; Fripiat et al., 2007), which enabled us to separate the different phases (brine vs. pure ice) by their melting point. This method relies on the fact that the brine drains faster than the pure ice crystal matrix melts. Therefore, the interconnected brines drain first, while less saline fractions, as the pure ice melts, are collected at the end. Bulk properties were computed using the weighted averages of the four sequential fractions. For clarity, the discussion is focused primarily on these bulk properties rather than the sequential fractions. The sequential fractions are used when addressing the potential bias induced by osmotic shock during ice sample melting (Text S1; Figure S1).

At Davis station, the ice core for salinity and biogeochemical measurements was sectioned directly after coring and pieces were stored in the dark in acid-cleaned plastic containers for transportation to the station-based laboratory. The samples were left to melt in the dark at room temperature, and salinity was measured after complete melting (Thermo Fisher Scientific Inc. 125A Plus). Subsamples for nutrients (NO_3^-, NO_2^-, NH_4^+, PO_4^{3-}, $Si(OH)_4$) were filtered using prerinsed syringe filters (0.2 μm porosity; Pall Acrodisc, Port Washington, NY, USA) and stored in acid-washed, prerinsed 60-ml polypropylene bottles at −20 °C. The remaining volume was filtered immediately through precombusted GF/F filters (0.7 μm porosity, Whatman) for POC and PON analysis. Filters were dried overnight at 50 °C and stored at room temperature.

The bottom 10-cm portion of the sea ice was sectioned at high resolution for two cores from the YROSIAE campaign (stations 9 and 10) and two cores sampled during the campaign at Davis Station (stations 2 and 5). These cores were stored at −30 °C in the dark at the home-based laboratory (Université libre de Bruxelles) before further processing. The bottom 10 cm were then cut in 1-cm sections and processed and analyzed following the same methods and protocols as described above for each sampling location.

2.3. Analytical methods

Measurements used as proxies for biomass (POC, PON, and $bSiO_2$) were completed at the home-based laboratory (Vrije Universiteit Brussel, Belgium). For POC and PON analysis, filters were placed overnight in acid (hydrochloric acid) fumes to remove carbonates. Filters were packed carefully in precombusted (24 h at 450 °C) silver cups suited for the autosampler. Carbon and nitrogen content were analyzed using an elemental analyzer (EA, Eurovector, Pavia, Italy) coupled to an isotope ratio mass spectrometer (IRMS, Delta V, Thermo Fisher Scientific Inc.; Roukaerts et al., 2016). Analysis for $bSiO_2$ and LSi followed Ragueneau et al. (2005), where polycarbonate membranes were submitted to a series ($n = 3$) of wet-alkaline digestions with 4 ml of 0.2 mol L^{-1} NaOH solution (pH 13.3) at 100 °C for 40 min. Following this step, another wet-acid digestion was performed with 0.2 ml of 2.9 M HF, allowing to react for 3 days. During the first digestion, most of the $bSiO_2$ is dissolved together with a fraction of the LSi. During the second digestion, the remaining $bSiO_2$ is dissolved still with a fraction of LSi. The third digestion is dedicated to measuring the Si:Al ratio of LSi to correct for the contribution of LSi in the two previous digestions. The fourth digestion is to dissolve LSi completely. Both Si and Al were measured using a sector-field ICP-MS (Element2, Thermo Fisher Scientific Inc.) as described in Fripiat et al. (2012).

Nutrient concentrations (NO_3^-, NO_2^-, PO_4^{3-}, NH_4^+, $Si(OH)_4$) were measured via colorimetry at the home-based laboratory (Vrije Universiteit Brussel, Belgium) using a continuous segmented flow auto-analyzer QuAAtro39 (Seal Analytical, Southampton, United Kingdom). The salinity of the standard solutions was adjusted to 6 for sea-ice samples. Regarding the YROSIAE samples, $Si(OH)_4$ measurements were performed on samples stored both frozen and at ambient temperature. There have been some concerns in the community that $Si(OH)_4$ polymerizes in frozen samples, inducing a bias when working with frozen samples (Zhang and Ortner, 1998); indeed, our comparison between frozen and ambient storage supports that $18 \pm 11\%$ of $Si(OH)_4$ was polymerized in the frozen samples. For nutrient concentrations only, a salinity normalization was applied, based on seawater and sea-ice

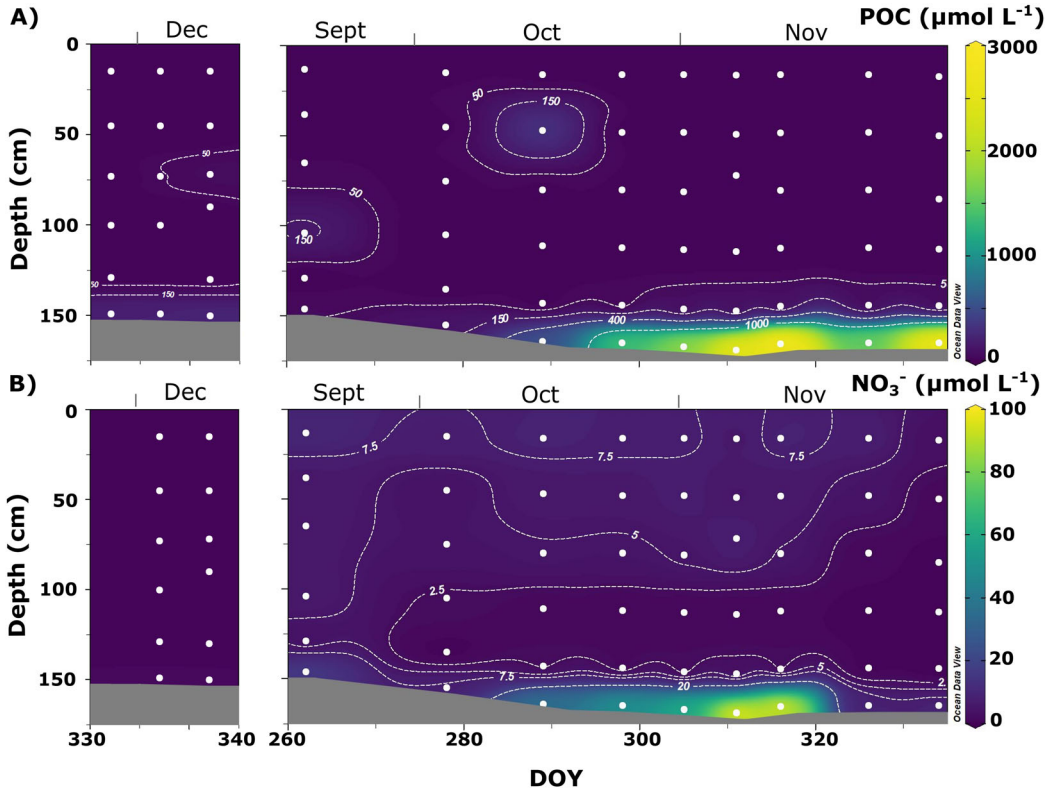

Figure 3. Seasonal evolution of biomass and nitrate in Antarctic landfast sea ice at Cape Evans. Vertical distribution of (A) bulk particulate organic carbon (µmol L^{-1}) and (B) bulk nitrate (NO_3^-, µmol L^{-1}) versus time in day of year at Cape Evans (YROSIAE). White dots are data points from field sampling. DOI: https://doi.org/10.1525/elementa.2020.00134.f3

bulk salinity, to allow an easy comparison of concentrations between sea ice and underlying seawater (Fripiat et al., 2017).

3. Results

3.1. Physical parameters

The sea-ice thickness at Cape Evans (YROSIAE) was 151 cm in late winter (September 19, YROSIAE-2) and gradually increased during early spring. A maximal thickness of 173 cm was reached on November 7, with ice thickness then remaining relatively constant until the end of the YROSIAE-2 sampling period (November 30; **Figure 3**). The three stations that were sampled during YROSIAE-1 had a smaller ice thickness of 154 cm. Ice textures were a combination of more granular/columnar ice at the top, a section of columnar ice in the center, and consolidated platelet/columnar ice in the lower parts (Carnat et al., 2014). Snow cover was low for all stations (<4 cm). Ice thickness at Davis Station was constant, around 158 cm, during the sampling period and consisted of mostly granular ice at the top and columnar ice in the interior and bottom of the ice (Lim et al., 2019). Snow cover was variable (5–25 cm). Ice thickness at Dumont d'Urville was around 70 cm in June and gradually increased to 154 cm at the end of November. The ice texture consisted of granular ice near the surface, a large section of columnar ice in the center, and consolidated platelet ice at the bottom (Fripiat et al., 2015). Snow cover was variable (0–40 cm). For all three locations, a transition was observed in the temperature profiles, with strong gradients from −2 °C at the ice-seawater interface to much lower values at the surface (down to −20 °C) at the beginning of the sampling period to nearly isothermal profiles at the end. Coinciding with the change in temperature was a decrease in sea-ice bulk salinities (Carnat et al., 2014; Fripiat et al., 2015; Lim et al., 2019; Van der Linden et al., 2020).

3.2. Biogeochemical parameters

The distribution of biomass in the sea ice is similar for the three locations, as represented by POC at YROSIAE (**Figure 3A**). Biomass was low in the surface and interior of the ice, and most of the biomass in spring was concentrated at the ice bottom. Focusing on the bottom ice section (10 cm) at the ice-seawater interface, the results for POC, PON, and $bSiO_2$ (shown in **Figure 4**; data in Table S1) are similar between the different time series. For YROSIAE-2 and DDU, POC concentrations increased rapidly during the growth season (September–November), reaching 2,600 and 1,000 µmol L^{-1}, respectively. A similar trend was reported for PON concentrations (reaching 260 and 160 µmol L^{-1}, respectively). Although not completely proportional to POC and PON, $bSiO_2$ concentrations in the bottom section also increased to 920 µmol L^{-1} during the growth season (YROSIAE-2). A sharp decrease was observed for the last two stations of YROSIAE-2, which was not clear for POC and PON. Late spring samples for YROSIAE collected in the preceding year (YROSIAE-1) had

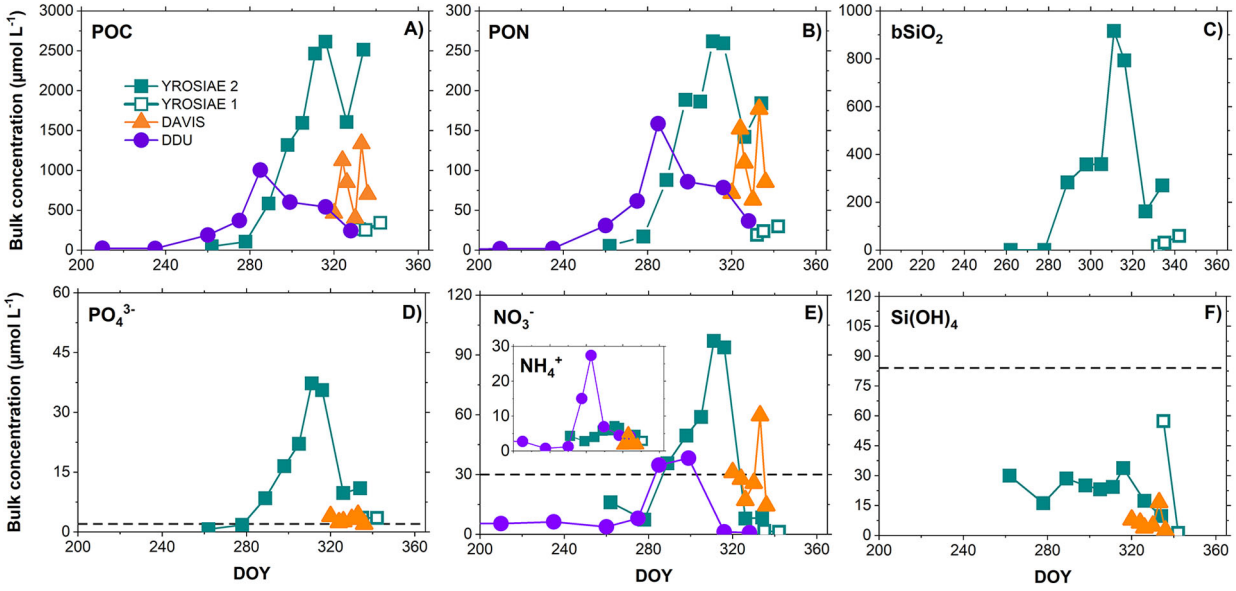

Figure 4. Seasonal evolution of biogeochemical parameters in Antarctic bottom landfast sea ice for three time series. Parameter concentrations in the bottom 10-cm ice section, plotted against day of year on the *x*-axis for sampling sites YROSIAE-1 (solid blue-green squares), YROSIAE-2 (open blue-green squares), DDU (solid purple circles), and DAVIS (solid orange triangles). Bulk concentrations of (A) particulate organic carbon (µmol L^{-1}), (B) particulate organic nitrogen (µmol L^{-1}), (C) biogenic silica (µmol L^{-1}), (D) phosphate (PO_4^{3-}, µmol L^{-1}), (E) nitrate (NO_3^-, µmol L^{-1}) with insert ammonium (µmol L^{-1}), and (F) silicate ($Si(OH)_4$, µmol L^{-1}). Black dashed lines represent underlying seawater values for the primary nutrients PO_4^{3-}, NO_3^-, and $Si(OH)_4$, referenced as the nutrients that are abundant in seawater and end products of remineralization/dissolution. DOI: https://doi.org/10.1525/elementa.2020.00134.f4

lower and relatively constant biomass at the bottom. At DDU, biomass decreased continuously toward the end of the sampling period. Sampling at Davis started when biomass was already elevated and large variations are reported between sampling days (between 460 and 1,300 µmol L^{-1} for POC, and 63 and 180 µmol L^{-1} for PON), possibly due to spatial variability.

At YROSIAE and DDU, nitrate and phosphate concentrations followed the accumulation of biomass (**Figures 3** and **4**; data in Table S1), with salinity-normalized concentrations early in the season close to seawater values (i.e., 30 µmol L^{-1} and 2 µmol L^{-1} for nitrate and phosphate, respectively; see Figure S2 for salinity-normalized nutrient concentrations in the bottom ice sections). At the peak of the bloom, bulk and salinity-normalized concentrations largely exceeded seawater concentrations. After the peak of the bloom, bulk NO_3^- and PO_4^{3-} concentrations decreased sharply. This sharp decrease coincides with the opening of the brine network through the full thickness of the ice, following the increase in surface temperature and leading to episodic full-depth convection within the sea ice. High and variable NO_3^- concentrations were reported at Davis, with lower and more stable PO_4^{3-} concentrations. However, bulk and salinity-normalized PO_4^{3-} concentrations at Davis (up to 4.3 µmol L^{-1} and 21 µmol L^{-1}, respectively) were still exceeding seawater value. Nitrite concentrations in bottom ice represented less than 5% of the $NO_3^- + NO_2^-$ concentrations (median contribution = 0.8%) and, therefore, are not discussed further in this article. Bulk NH_4^+ concentrations ranged between 0.8 µmol L^{-1} and 27 µmol L^{-1}, following the seasonal trend that was observed for NO_3^-, PO_4^{3-}, and biomass.

$Si(OH)_4$ concentrations did not accumulate as strongly as observed for NO_3^- and PO_4^{3-}, with a maximum bulk concentration of 34 µmol L^{-1} at the peak of the bloom (YROSIAE-2; **Figure 4**), corresponding to a salinity-normalized concentration of 130 µmol L^{-1}. Except for some sporadic small accumulations, no seasonal increase or decrease in $Si(OH)_4$ concentrations was detected, unlike the NO_3^- and PO_4^{3-} accumulations discussed above. There is one outlier during YROSIAE-1, after the algal bloom, with a bulk $Si(OH)_4$ concentration of 57 µmol L^{-1} and salinity-normalized $Si(OH)_4$ concentration of 480 µmol L^{-1}, up to 6-fold the seawater concentration (84 µmol L^{-1}).

High-resolution profiles of nutrients and biomass for the bottom 10 cm of sea ice are presented in **Figure 5**. Intense vertical gradients are reported with most of the biomass accumulation being observed in the lower 3 cm of the ice, close to the ice-water interface, with POC concentrations reaching 25,000 µmol C L^{-1}. POC and PON concentrations progressively decreased higher in the ice, reaching a low of 67 µmol C L^{-1}, with a sharper decline with increasing distance from the ice-seawater interface at Davis compared to YROSIAE. One core at Davis presented a maximum in biomass at 3 cm above the interface. This maximum was also visible as a green/brown layer in the core (Figure S3). As observed for the time series described above, the accumulation of biomass coincided with the accumulation of NO_3^- and PO_4^{3-}, with bulk concentrations up to 190 and 120 µmol L^{-1} near the ice-water

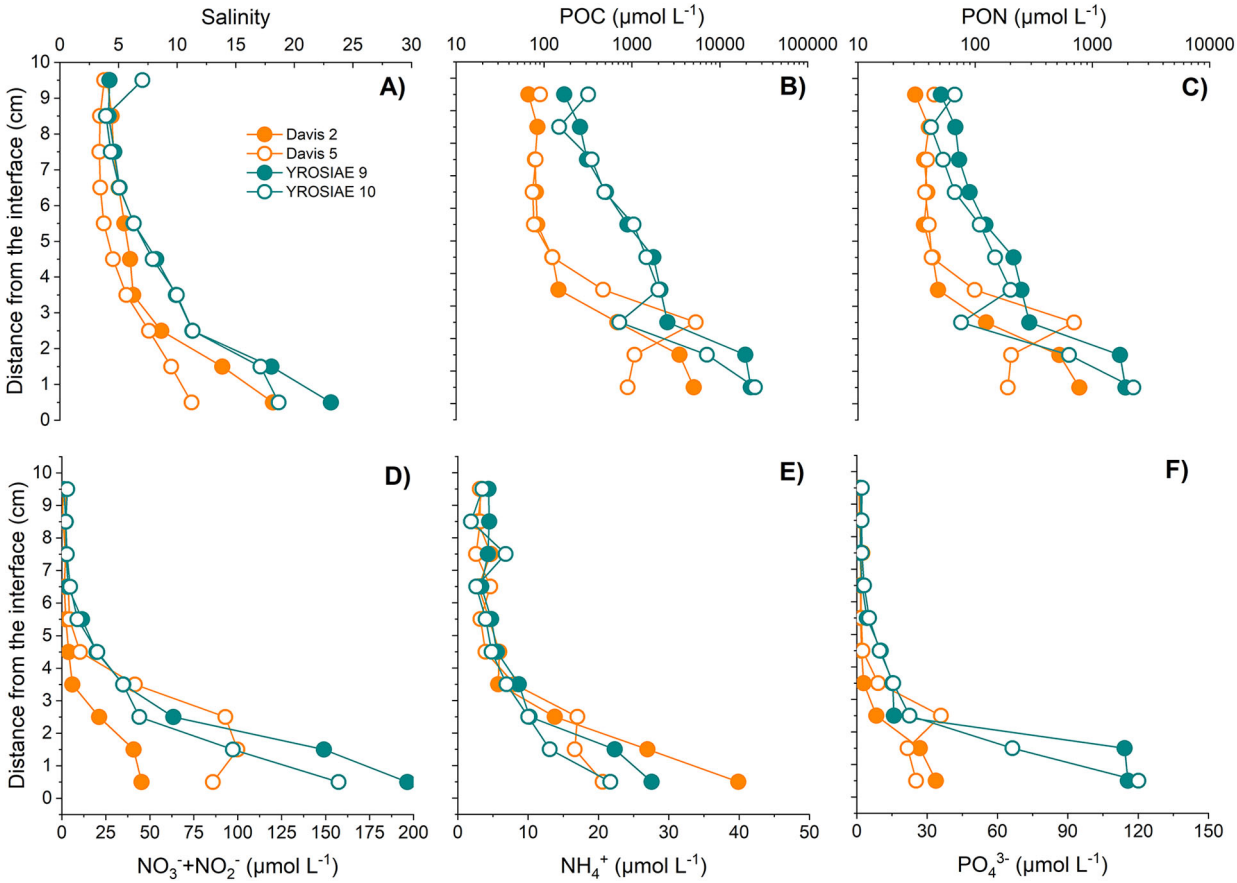

Figure 5. High resolution profiles of biogeochemical parameters in the bottom 10 cm of landfast sea ice. Two ice cores sampled during the YROSIAE campaign and two ice cores from Davis Station were sectioned in 1-cm slices at the home-based laboratory (Université libre de Bruxelles) and analyzed for salinity and concentrations of particulate organic carbon (POC), particulate organic nitrogen (PON), nitrate plus nitrite, ammonium, and phosphate. A logarithmic scale was used for POC and PON to condense the large concentration differences observed in the bottom 10 cm; interface refers to the ice-seawater interface (0 cm). DOI: https://doi.org/10.1525/elementa.2020.00134.f5

interface, respectively. Higher in the ice, NO_3^- and PO_4^{3-} decreased rapidly to near exhaustion at approximately 5 cm above the interface. Ammonium (NH_4^+) followed a similar trend with concentrations ranging between 10 and 40 µmol L^{-1} in the lower 3 cm and decreasing toward 5 µmol L^{-1} higher in the ice. These high-resolution profiles are in line with those previously obtained in Arctic landfast sea ice (Smith et al., 1990), where bulk NO_3^- and PO_4^{3-} concentrations reached 400 and 70 µmol L^{-1}, respectively, near the ice-water interface. The results from these high-resolution profiles further support the tight coupling between nutrients and biomass.

4. Discussion

4.1. Biogeochemical dynamics in Antarctic bottom landfast ice

During the growth season, high biomass was observed at the three landfast ice sampling sites. Both YROSIAE and DDU data sets show a large seasonal increase in biomass in the bottom 10 cm of the cores, with the accumulation at DDU starting roughly 1 month earlier than at YROSIAE (**Figures 3** and **4**). The difference in latitude between the two locations, and consequent difference in seasonal irradiance, allowed for an earlier start of autotrophic growth at DDU. Another aspect is the much lower snow thicknesses at YROSIAE (<4 cm) compared to both DDU and Davis (<40 cm). Thinner snow allows for more light to penetrate through the ice cover (Mundy et al., 2005; Leu et al., 2015; Meiners et al., 2018) and, therefore, may also help to explain the larger accumulation of biomass at YROSIAE (**Figure 4**). The rapid decrease of biomass in late spring may be linked to either a loss of habitat through bottom ablation or a deterioration in environmental conditions (e.g., light, nutrients, and mortality). The seasonal increase in biomass at the bottom of sea ice agrees with the evolution in dissolved inorganic carbon (DIC) and molecular oxygen (O_2) at YROSIAE (Figure S4). It is indicative of a net autotrophic system with consumption of DIC and production of O_2 during the growth season (September–November) and a net heterotrophic system with production of DIC and consumption of O_2 in late spring (Van der Linden et al., 2020).

Inorganic nutrients are essential to ice algal growth, but the nutrient stock in early spring is insufficient to

support the observed biomass accumulation later in the season. Hence, additional nutrients must be supplied via convection and/or diffusion from the underlying seawater in order to support the biomass accumulation that is observed (Cota et al., 1987; Fripiat et al., 2014a; Fripiat et al., 2015). Coinciding with the seasonal peak in biomass, a strong accumulation in NO_3^- and PO_4^{3-} was observed in the bottom ice layer (**Figures 3** and **4**). This large accumulation is common in bottom landfast sea ice (Smith et al., 1990; Arrigo et al., 1995; Gunther and Dieckmann, 1999; Thomas and Dieckmann, 2002; Cozzi, 2008; van der Merwe et al., 2011; Riaux-Gobin et al., 2013; Lannuzel et al., 2014; Fripiat et al., 2015) and in pack ice (Fripiat et al., 2017, and references therein). High nutrient concentrations in sea ice are considered to result from heterotrophic bacterial activity or from excretion by metazoan grazers (Gradinger and Ikävalko, 1998; Fripiat et al., 2015). The release of internal nutrient pools due to cell lysis can also cause an increase in nutrient concentrations. This release can be the result of sloppy feeding by zooplankton, viral lysis, or osmotic shock during sampling. Cell lysis due to an osmotic shock from sampling was avoided in our study by applying a sequential melting procedure for the YROSIAE bottom samples (Text S1).

In general, a combination of factors is assumed to be responsible for the occurrence of these accumulations in nutrients, but their mere occurrence requires that the production of nutrients exceeds consumption. Conventional explanations are insufficient to explain a continuously increasing nutrient concentration while biomass is still increasing. Intuitively, one would expect an inverse coupling as ice algae consume nutrients to sustain their growth. The absence of inverse coupling leads us to conclude that there is a "nutrient paradox" in the biogeochemical observations of Antarctic bottom fast ice reported here that cannot be explained adequately within the current nutrient paradigm (**Figure 1A**).

4.2. Solving the nutrient paradox

To gain insight into the interactions at play, we implemented a conceptual NPZD model (see Supplemental Materials for model description and sensitivity: Text S2, Table S2). The aim of the model is not to create a digital twin of the sea-ice environment but to explore which mechanisms and processes are required to explain the observations. The model is based on nitrogen, for which both organic and inorganic concentrations were measured in the field. We focused on the time series at Cape Evans (YROSIAE) as this study had the most complete data set. As DON was not measured at YROSIAE, total organic nitrogen content (TON = DON + PON) could not be calculated. DON data from DDU accounted on average for one half of the TON (Fripiat et al., 2015), which suggests that the concentration of TON at YRSOSIAE was likely even higher than observed solely based on PON concentrations. Field observations for PON correspond to the combination of all organic nitrogen pools (P, Z, D) in the model, while dissolved inorganic nitrogen (DIN = $NO_3^- + NO_2^- + NH_4^+$) corresponds to the nutrient pool (N) in the model. Bulk

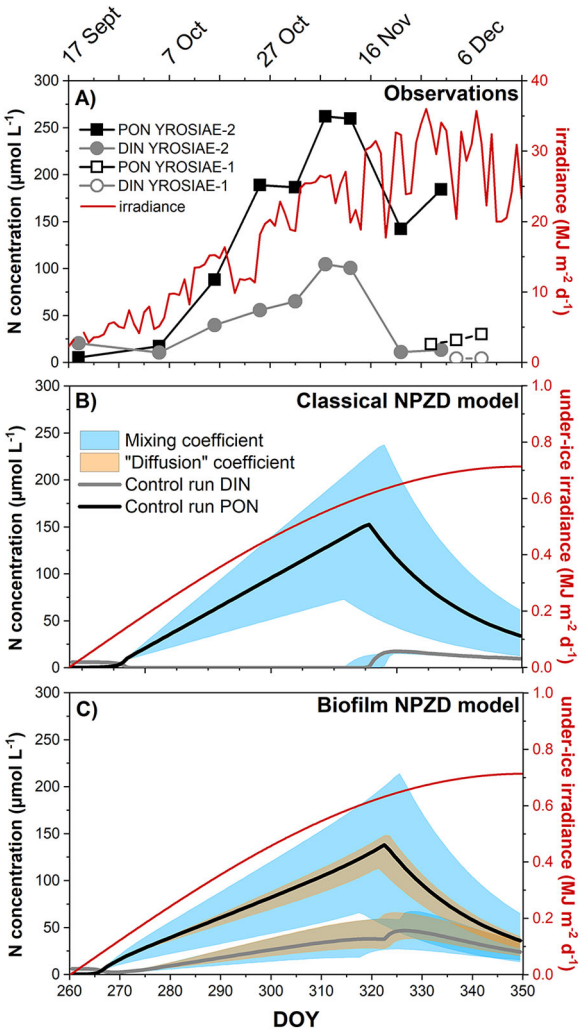

Figure 6. Seasonal evolution of the observations compared to two conceptual nutrient-phytoplankton-zooplankton-detritus (NPZD) models, classical and biofilm-based. Observations (A) and two conceptual models (B, C) for biomass and nutrients in landfast sea ice. (A) Observations from the YROSIAE campaign for particulate organic nitrogen (PON) and dissolved inorganic nitrogen (DIN = $NO_3^- + NO_2^- + NH_4^+$) follow a similar seasonal trend with increasing bulk concentrations as irradiance increases. (B) NPZD model output for the current (classical) paradigm (**Figure 1A**) cannot reproduce observations because DIN-modeled concentrations decrease from low to negligible values during the bloom period. (C) By implementing the NPZD model with a spatial decoupling for the N-pool at the microscale due to the biofilm (**Figure 1B**), both PON and total DIN concentrations in the bottom section can increase as observed during the field sampling. In (B) and (C), the sensitivity to exchange between brine and seawater (blue) and to exchange between brine and water in the biofilm (orange) is shown with the envelopes, that is, by increasing and decreasing the mixing coefficients (i.e., K_{mixing} and K_{diff}, respectively) by 50% as compared to the control run (see Supplementary Materials for a more complete sensitivity analysis). DOI: https://doi.org/10.1525/elementa.2020.00134.f6

concentrations of PON and DIN for YROSIAE, shown in **Figure 6A**, are in line with observations at DDU and Davis.

In our current understanding of the sea-ice nitrogen cycle (i.e., classical NPZD model), DIN is supplied from the underlying seawater and consumed by autotrophs to sustain biomass growth (**Figure 1A**). Hence, DIN and PON are inversely proportional during the growth phase (**Figure 6B**). The continuous supply and assimilation of DIN into the ice results in a biological "pumping" effect and explains the large accumulation of biomass in bottom landfast sea ice (Cota et al., 1987; Fripiat et al., 2014a; Fripiat et al., 2015). Autotrophs can be consumed, in turn, by small and larger consumers. Subsequently, living cells become detrital matter due to cell lysis, grazing, and/or viral infections. This detrital matter is then remineralized by heterotrophic bacteria and released as nutrients. The released nutrients can again be consumed by growing algae or lost to the underlying seawater. Hence, early in the season, there is a net assimilation of nutrients into biomass, leading to depleted nutrient conditions (**Figure 6B**). Later in the bloom period, when mortality increases and growth conditions are less optimal, biomass concentrations decrease. When the production of inorganic nutrients by remineralization is larger than the assimilation for growth, nutrients can start to accumulate (**Figure 6B**). During this transition period, a combination of high biomass and high nutrient concentrations can be expected. This temporal decoupling between net assimilation and remineralization of nutrients could explain field observations for short time series where sampling starts when the bloom is already developed, such as at Davis Station. However, field observations at Cape Evans (YROSIAE campaign) and Dumont d'Urville started before this transition and show no time delay between dissolved nutrient buildup and biomass accumulation (**Figures 4** and **6a**). Overall, the observations do not fit the classical conceptual model in **Figure 1A**. We suggest that this misfit results from the fact that the bottom sea-ice environment is not a simple matrix in which algae and nutrients are distributed homogeneously within the brine network.

We consider that the possibility of spatial decoupling, allowing a trophic gradient between autotroph-dominated and heterotroph-dominated communities, offers an alternative to a temporal decoupling. In this case, autotroph-dominated communities accumulate biomass with a net assimilation of nutrients, while decaying biomass is remineralized in adjacent, spatially separated, heterotroph-dominated communities. If nutrient consumption is lower than remineralization in the heterotroph-dominated communities, nutrients can accumulate locally. The observations in bulk sea-ice samples could thus consist of a mixture of these two spatially separated, contrasting environments and lead to the apparent accumulation of both biomass and nutrients in a single 10-cm thick bottom ice sample. Such a trophic gradient might take place in the vertical, with net assimilation at the ice-seawater interface where most of the biomass is observed. Here, nutrients are consumed by ice algae and nutrient concentrations are below seawater levels. Simultaneously, biomass could be remineralized in a layer a few centimeters above the ice-water interface with net remineralization where nutrients would accumulate and exceed seawater levels. To test this hypothesis, two ice cores from the YROSIAE campaign and two cores sampled at Davis Station were sectioned at higher resolution (1 cm) over the bottom 10 cm. In disagreement with the above hypothesis, results show a strong positive relationship at the centimeter scale between nutrients and biomass. The largest accumulations for both biomass and nutrients are observed near the ice-water interface. In contrast, low nutrient concentrations, associated with low biomass, are observed a few centimeters above the interface (**Figure 5**), as also described in Arctic landfast sea ice (Smith et al., 1990).

The spatial segregation should therefore occur on a smaller scale with spatial trophic gradients at the subcentimeter scale. Hence, environments with a net assimilation of nutrients would coexist in close proximity with environments where remineralization exceeds assimilation. In sea ice, high concentrations of gel-like EPS are commonly reported, and the microbial community has been observed to be embedded preferentially in a biofilm (Krembs et al., 2002; Krembs et al., 2011; Meiners et al., 2003, 2004, 2008; Krembs and Deming, 2008; Underwood et al., 2010; Ewert and Deming, 2013). Here, we have defined a biofilm as an aggregate of microorganisms in which cells that are frequently embedded within a self-produced matrix of EPS adhere to each other and/or to a surface (Vert et al., 2012; Flemming et al., 2016). A biofilm can induce a spatial gradient at subcentimeter scale by clogging the brine network or by inducing biogeochemical and physiological heterogeneity within the biofilm. By clogging the brine network (Krembs and Deming, 2008; Krembs et al., 2011), isolated liquid brine pockets may form where decaying organic matter is remineralized. If remineralization exceeds nutrient assimilation in these isolated subsystems, it will lead to a local accumulation of nutrients. Assimilation and remineralization gradients may also occur within the biofilm, in which case the biogeochemical and physiological heterogeneity arises as the biofilm develops. Such gradients are a result of reaction–diffusion interactions for metabolic substrates by distinct microbial communities inhabiting different layers in the biofilm (Stewart and Franklin, 2008). In the early stage, the biofilm is thin and metabolic substrates and products are readily transported through it by diffusion. As the biofilm thickens, diffusion can no longer supply substrates deeper in the biofilm. In these deeper layers, algal growth will cease and cells may be expected to die. When the generation of metabolic products from respiration exceeds the loss by diffusion through the biofilm, nutrients can accumulate deep inside the biofilm.

To test this hypothesis, the small-scale spatial decoupling between assimilation and remineralization of nutrients was implemented in the conceptual NPZD model by splitting the nutrient pool into $N_{biofilm}$ and N_{brines} (**Figure 1B**). The $N_{biofilm}$ pool is "supplied" by DIN from a heterotrophic community located in microenvironments, either deep inside the biofilm (Stewart and Franklin, 2008) or physically isolated by the clogging of a fraction of the

brine network (Krembs et al., 2011). Here, nutrients can accumulate if production by remineralization exceeds the loss by diffusion because the nutrients are not readily accessible for assimilation. The N_{brines} pool represents nutrients in the liquid brines in contact with the biofilm and with the brine network directly in contact with the underlying seawater supplying DIN into the ice. In this case, bulk nutrient concentrations measured in bottom ice samples are a mixture of these two pools. The field observations of DIN accumulation, coinciding with increasing biomass, can be reproduced easily by introducing a small-scale spatial decoupling in the NPZD model (**Figure 6C**). We, therefore, suggest that the nutrient paradox commonly reported in productive sea ice is generated by coexisting contrasting microenvironments at the subcentimeter scale, owing to the presence of a biofilm (**Figure 1B**).

4.3. Mechanisms and implications

A complete decoupling between DIN assimilation and DIN production in the model is likely an oversimplification. Moreover, the model uses DIN as a nutrient, although DIN is the sum of NO_3^-, NO_2^-, and NH_4^+ which are produced and consumed in distinct microbial processes. Organic matter in sea ice is remineralized to NH_4^+ (Reidel et al., 2007), which in turn can be adsorbed onto EPS or decaying organic matter embedded in the ice (Fripiat et al., 2017). This NH_4^+ can be assimilated into biomass or converted to NO_3^- by nitrifiers, known to be active in sea ice (Fripiat et al., 2014a; Fripiat et al., 2015; Baer et al., 2015; Firth et al., 2016) and to thrive in biofilms by forming cooperative communities involved in the different nitrification steps (Hagopian and Riley, 1998). The NO_3^- and NH_4^+ produced, either in the deeper layers of the proposed biofilm or in isolated liquid brine pockets, can then diffuse toward microenvironments where there is a net assimilation of nutrients, either at the biofilm–brine interface or in the brine network directly in contact with the underlying seawater. A nutrient gradient is likely to be established, with autotrophic growth supported by NO_3^- from brines (i.e., underlying seawater for which NO_3^- is the main dissolved inorganic N constituent) and from heterotroph-dominated microenvironments (i.e., NH_4^+ and NO_3^- being generated by remineralization and nitrification, respectively). If the consumption of O_2 by heterotrophic respiration is large enough, O_2 can become depleted in some of these microenvironments. If diffusion of O_2 from the seawater and brines is insufficient, anoxic zones might develop. Anoxic microenvironments in the bottom 3 cm of sea ice have been reported in the Arctic with the occurrence of anoxic processes such as denitrification and anammox (Rysgaard et al., 2008).

Like NO_3^-, the concentrations of PO_4^{3-} showed an increase during the bloom. However, the relative increase in PO_4^{3-} is even larger than for NO_3^-. The N/P ratio in the dissolved phase (DIN/PO_4^{3-}) decreases to 3 at the peak of the bloom and continues to decrease to 1 after the bloom. Although a low N/P-uptake ratio by sea-ice algae might play a role, an uptake ratio below 5 has not been reported in the literature (Arrigo, 2005; Martiny et al., 2013). An increased retention of PO_4^{3-} in the biofilm due to the formation of weak metal-organic complexes with EPS can decrease the diffusion rate of PO_4^{3-} and result in a larger accumulation compared to NO_3^- (Maranger and Pullin, 2003; Fripiat et al., 2017). Additionally, if anoxic zones are present in a sea-ice biofilm (Rysgaard et al., 2008), denitrification could take place and consume part of the produced NO_3^- with a resulting small production of PO_4^{3-} (Gruber and Sarmiento, 1997).

In contrast with NO_3^- and PO_4^{3-} and despite a large concentration variability, there is no clear trend in $Si(OH)_4$ concentrations over the bloom period, hence no obvious accumulation of $Si(OH)_4$. At the same time, a large increase in $bSiO_2$, up to three times larger than the PON accumulation, is observed. The absence of clear $Si(OH)_4$ trends, with salinity-normalized values oscillating around seawater concentrations (Figure S2f), in the presence of a large accumulation of $bSiO_2$ already indicates that the recycling of silicon in sea ice is occurring but is rather limited. Dead diatoms are likely embedded in the sea-ice biofilm where their silicon frustules would be prone to dissolution (Bidle and Azam, 1999; Fripiat et al., 2014b). However, the physical dissolution of silicon frustules may be slow, given the prevailing low temperature conditions, implying a lesser impact of this recycling process on $Si(OH)_4$ concentrations. In addition, no absorption of $Si(OH)_4$ is expected onto decaying organic matter (Fripiat et al., 2017).

To conclude, the observations of simultaneous accumulations for nutrients and biomass in biologically productive sea ice can be explained by a spatial decoupling between net assimilation and net remineralization of nutrients at the subcentimeter scale. By creating chemical gradients, biofilms could create and host microenvironments with contrasting microbial communities within the brine network. Both EPS and embedded decaying organic matter may also favor nutrient (PO_4^{3-} and NH_4^+) adsorption, thereby maintaining remineralization products close to the sympagic community. By retaining water and slowing diffusion, biofilms ensure that nutrients can accumulate without being lost, either deeper in the biofilm or in isolated liquid brine pockets being formed by the clogging of the brine network. Meanwhile, exchanges between the brines and the underlying seawater can supply more nutrients into the ice by convection and diffusion. Although not directly observed in this study, biofilms help to explain other peculiar observations in high biomass sea-ice environments, such as iron accumulation, alkalinity excess, the precipitation of calcium carbonate, and the occurrence of denitrification and anammox (Rysgaard et al., 2008; Lannuzel et al., 2016; Van der Linden et al., 2020). The central role of biofilms in sea-ice biogeochemistry requires further study, but the enabling of contrasting processes to take place on a small spatial scale has far-reaching implications for our understanding of this complex ecosystem.

Data accessibility statement

Data used in these analyses are available in the Supplemental Materials (Table S1).

Supplemental files

The supplemental files for this article can be found as follows:

Tables S1–2. Text S1–2. Figures S1–6. PDF

Acknowledgments

Our warm thanks go to B. Staite, C. Robineau, G. Massé, J. Zhou, V. Schoemann, T. Goossens, W. Champenoix, J. Janssens, N. Kanna, K. Meiners, M. Milnes, the Scott Base crew, the crew at Davis Station, the crew at Dumont D'Urville, and the French Polar Institute (IPEV) for their assistance and logistic support during field work. We are grateful to D. Verstraeten for the lab management at the Vrije Universiteit Brussel, to M.A. Weigand and S. Oleynik for the lab management at Princeton University, and to S. El Amri for the lab management at the Université Libre de Bruxelles.

Funding

This research was supported by the Belgian Federal Science Policy (BIGSOUTH network, SD/CA/05A of SPSDIII, Support Plan for Sustainable Development, and OCeANIC project, BL/12/C63), the FRS-FNRS (project YROSIAE, contract 2.451711), the Antarctic New Zealand (project K131), the Australian Antarctic Science (AAS) project no. 4291 (D. Lannuzel), and the French Polar Institute (ICELIPIDS, project 1010). Florian Deman is PhD student supported by the Belgian Federal Science Policy Office (OCeANIC project, BL/12/C63). F. Van der Linden and B. Delille are PhD student and research associate, respectively, of the F.R.S.-FNRS. G. Carnat benefited from a Belgian FNRS research grant (contract A 4/5 – MCF/DM – 2657). D. Lannuzel is an Australian Council Future Fellow supported by grant L0026677.

Competing interests

The authors declare that there are no competing financial or personal interests in relation to the work described.

Author contributions

Contributed to conception and design: AR, FF.

Contributed to acquisition of data: AR, FD, FVDL, GC, SM, DL, BD, J-LT, FF.

Contributed to analysis and interpretation of data: AR, FD, FF.

Drafted the article: AR, FF.

Revised the article: AR, FD, FVDL, GC, AB, SM, DL, FD, BD, J-LT, FF.

Approved the submitted version for publication: AR, FD, FVDL, GC, AB, SM, DL, FD, BD, J-LT, FF.

References

Arrigo, KR. 2005. Marine microorganisms and global nutrient cycles. *Nature* **437**: 349–355. DOI: https://dx.doi.org/10.1038/nature04159.

Arrigo, KR, Dieckmann, GS, Gosselin, M, Robinson, DH, Fritsen, CH, Sullivan, CW. 1995. High resolution study of the platelet ice ecosystem in McMurdo Sound, Antarctica: Biomass, nutrient, and production profiles within a dense microalgal bloom. *Marine Ecology Progress Series* **127**(1–3): 255–268. DOI: https://dx.doi.org/10.3354/Meps127255.

Baer, SR, Connelly, TL, Bronk, DA. 2015. Nitrogen uptake dynamics in landfast sea ice of the Chukchi Sea. *Polar Biology* **38**: 781–797. DOI: https://dx.doi.org/10.1007/s00300-014-1639-y.

Becquevort, S, Dumont, I, Tison, J-L, Lannuzel, D, Sauvée, ML, Chou, L, Schoemann, V. 2009. Biogeochemistry and microbial community composition in sea ice and underlying seawater off east Antarctica during early spring. *Polar Biology* **32**(6): 879–895. DOI: https://dx.doi.org/10.1007/s00300-009-0589-2.

Bidle, KD, Azam, F. 1999. Accelerated dissolution of diatom silica by marine bacterial assemblages. *Nature* **397**(6719): 508–512. DOI: https://dx.doi.org/10.1038/17351.

Bowman, JS. 2015. The relationship between sea ice bacterial community structure and biogeochemistry: A synthesis of current knowledge and known unknowns. *Elementa: Science of the Anthropocene* **3**: 1–20. DOI: https://dx.doi.org/10.12952/journal.elementa.000072.

Carnat, G, Zhou, J, Papakyriakou, T, Delille, B, Goossens, T, Haskell, T, Schoemann, V, Fripiat, F, Rintala, J-M, Tison, J-L. 2014. Physical and biological controls on DMSP dynamics in ice shelf-influenced fast ice during a winter-spring and a spring-summer transitions. *Journal of Geophysical Research: Oceans* **119**(5): 2882–2905. DOI: https://dx.doi.org/10.1002/2013JC009381.

Cota, GF, Prinsenberg, SJ, Bennett, EB, Loder, JW, Lewis, MR, Anning, JL, Watson, NHF, Harris, LR. 1987. Nutrient fluxes during extended blooms of Arctic ice algae. *Journal of Geophysical Research* **92**(C2): 1951. DOI: https://dx.doi.org/10.1029/JC092iC02p01951.

Cozzi, S. 2008. High-resolution trends of nutrients, DOM and nitrogen uptake in the annual sea ice at Terra Nova Bay, Ross Sea. *Antarctic Science* **20**(05): 441–454. DOI: https://dx.doi.org/10.1017/s0954102008001247.

Eicken, H, Lange, MA, Dieckmann, GS. 1991. Saptial variability of sea-ice properties in the northwestern Weddell Sea. *Journal of Geophysical Research* **96**: 10603–10615.

Ewert, M, Deming, JW. 2013. Sea ice microorganisms: Environmental constraints and extracellular responses. *Biology (Basel)* **2**(2): 603–628. DOI: https://dx.doi.org/10.3390/biology2020603.

Firth, E, Carpenter, SD, Sørensen, HL, Collins, RE, Blum, JD. 2016. Bacterial use of choline to tolerate salinity shifts in sea-ice brines. *Elementa: Science of the Anthropocene* **1**: 4.

Flemming, H-C, Wingender, J, Szewzyk, U, Steinberg, P, Rice, SA, Kjelleberg, S. 2016. Biofilms: an emergent form of bacterial life. *Nature Reviews Microbiology* **14**(9): 563–575. DOI: https://dx.doi.org/10.1038/nrmicro.2016.94.

Fripiat, F, Cardinal, D, Tison, J-L, Worby, A, André, L. 2007. Diatom-induced silicon isotopic fractionation in Antarctic sea ice. *Journal of Geophysical Research: Biogeosciences* **112**(G02001). DOI: https://dx.doi.org/10.1029/2006JG000244.

Fripiat, F, Cavagna, A-J, Dehairs, F, de Brauwere, A, André, L, Cardinal, D. 2012. Processes controlling the Si-isotopic composition in the Southern Ocean and application for paleoceanography. *Biogeosciences* **9**(7): 2443–2457. DOI: https://dx.doi.org/10.5194/bg-9-2443-2012.

Fripiat, F, Meiners, KM, Vancoppenolle, M, Papadimitriou, S, Thomas, DN, Ackley, SF, Arrigo, KR, Carnat, G, Cozzi, S, Delille, B, Dieckmann, GS, Dunbar, RB, Fransson, A, Kattner, G, Kennedy, H, Lannuzel, D, Munro, DR, Nomura, D, Rintala, J-M, Schoemann, V, Stefels, J, Steiner, N, Tison, J-L. 2017. Macro-nutrient concentrations in Antarctic pack ice: Overall patterns and overlooked processes. *Elementa: Science of the Anthropocene* **5**: 13. DOI: https://dx.doi.org/10.1525/elementa.217.

Fripiat, F, Sigman, DM, Fawcett, SE, Rafter, PA, Weigand, MA, Tison, J-L. 2014a. New insights into sea ice nitrogen biogeochemical dynamics from the nitrogen isotopes. *Global Biogeochemical Cycles* **28**: 115–130. DOI: https://dx.doi.org/10.1002/2013GB004729.

Fripiat, F, Sigman, DM, Massé, G, Tison, J-L. 2015. High turnover rates indicated by changes in the fixed N forms and their stable isotopes in Antarctic landfast sea ice. *Journal of Geophysical Research* **120**(4): 3079–3097. DOI: https://dx.doi.org/10.1002/2014JC010583.

Fripiat, F, Tison, J-L, André, L, Notz, D, Delille, B. 2014b. Biogenic silica recycling in sea ice inferred from Si-isotopes: Constraints from Arctic winter first-year sea ice. *Biogeochemistry* **119**(1): 25–33. DOI: https://dx.doi.org/10.1007/s10533-013-9911-8.

Gradinger, R, Ikävalko, J. 1998. Organism incorporation into newly forming Arctic sea ice in the Greenland Sea. *Journal of Plankton Research* **20**(5): 871–886. DOI: https://dx.doi.org/10.1093/plankt/20.5.871.

Gruber, N, Sarmiento, JL. 1997. Global patterns of marine nitrogen fixation and denitrification. *Global Biogeochemical Cycles* **11**(2): 235–266. DOI: https://dx.doi.org/10.1029/97GB00077.

Gunther, S, Dieckmann, GS. 1999. Seasonal development of algal biomass in snow-covered fast ice and the underlying platelet layer in the Weddell Sea, Antarctica. *Antarctic Science* **11**(3): 305–315. DOI: https://dx.doi.org/10.1017/S0954102099000395.

Hagopian, DS, Riley, JG. 1998. A closer look at the bacteriology of nitrification. *Aquacultural Engineering* **18**(4): 223–244. DOI: https://dx.doi.org/10.1016/S0144-8609(98)00032-6.

Kaartokallio, H, Søgaard, DH, Norman, L, Rysgaard, S, Tison, JL, Delille, B, Thomas, DN. 2013. Short-term variability in bacterial abundance, cell properties, and incorporation of leucine and thymidine in subarctic sea ice. *Aquatic Microbial Ecology* **71**(1): 57–73. DOI: https://dx.doi.org/10.3354/ame01667.

Krembs, C, Deming, JW. 2008. The role of exopolymers in microbial adaptation to sea ice, in Margesin, R, Schinner, F, Marx, J, Gerday, C eds., *Psychrophiles: From biodiversity to biotechnology*. Berlin, Germany: Springer-Verlag: 247–264.

Krembs, C, Eicken, H, Deming, JW. 2011. Exopolymer alteration of physical properties of sea ice and implications for ice habitability and biogeochemistry in a warmer Arctic. *Proceedings of the National Academy of Sciences of the United States of America* **108**(9): 3653–3658. DOI: https://dx.doi.org/10.1073/pnas.1100701108.

Krembs, C, Eicken, H, Junge, K, Deming, JW. 2002. High concentrations of exopolymeric substances in Arctic winter sea ice: Implications for the polar ocean carbon cycle and cryoprotection of diatoms. *Deep Sea Research Part I: Oceanographic Research Papers* **49**(12): 2163–2181. DOI: https://dx.doi.org/10.1016/S0967-0637(02)00122-X.

Krembs, C, Gradinger, R, Spindler, M. 2000. Implications of brine channel geometry and surface area for the interaction of sympagic organisms in Arctic sea ice. *Journal of Experimental Marine Biology and Ecology* **243**(1): 55–80.

Lannuzel, D, Tedesco, L, van Leeuwe, M, Campbell, K, Flores, H, Delille, B, Miller, L, Stefels, J, Assmy, P, Bowman, J, Brown, K, Castellani, G, Chierici, M, Crabeck, O, Damm, E, Else, B, Fransson, A, Fripiat, F, Geilfus, N-X, Jacques, C, Jones, E, Kaartokallio, H, Kotovitch, M, Meiners, K, Moreau, S, Nomura, D, Peeken, I, Rintala, J-M, Steiner, N, Tison, J-L, Vancoppenolle, M, Van der Linden, F, Vichi, M, Wongpan, P. 2020. The future of Arctic sea-ice biogeochemistry and ice-associated ecosystems. *Nature Climate Change* **10**(11): 983–992. DOI: https://dx.doi.org/10.1038/s41558-020-00940-4.

Lannuzel, D, Vancoppenolle, M, van der Merwe, P, de Jong, J, Meiners, KM, Grotti, M, Nishioka, J, Schoemann, V. 2016. Iron in sea ice: Review and new insights. *Elementa: Science of the Anthropocene* **4**: 130. DOI: https://dx.doi.org/10.12952/journal.elementa.000130.

Lannuzel, D, van der Merwe, P, Townsend, AT, Bowie, AR. 2014. Size fractionation of iron, manganese and aluminium in Antarctic fast ice reveals a lithogenic origin and low iron solubility. *Marine Chemistry* **161**: 47–56. DOI: https://dx.doi.org/10.1016/j.marchem.2014.02.006.

Leu, E, Mundy, CJ, Assmy, P, Campbell, K, Gabrielsen, TM, Gosselin, M, Juul-Pedersen, T, Gradinger, R. 2015. Arctic spring awakening – Steering principles behind the phenology of vernal ice algal blooms. *Lithosphere Oceanography* **139**: 151–170. DOI: https://dx.doi.org/10.1016/j.pocean.2015.07.012.

Lim, SM, Moreau, S, Vancoppenolle, M, Deman, F, Roukaerts, A, Meiners, KM, Janssens, J, Lannuzel, D. 2019. Field observations and physical-biogeochemical modeling suggest low silicon affinity for

Antarctic fast ice diatoms. *Journal of Geophysical Research: Oceans* **124**(11): 7837–7853. DOI: https://dx.doi.org/10.1029/2018JC014458.

Maranger, R, Pullin, M. 2003. Elemental complexation by dissolved organic matter in lakes: Implications for Fe speciation and the bioavailability of Fe and P, in Findlay, S, Sinsabaugh, RL eds., *Aquatic ecosystems interactivity of dissolved organic matter*. London, UK: Academic Press: 185–216.

Martiny, AC, Pham, CTA, Primeau, FW, Vrugt, JA, Moore, JK, Levin, SA, Lomas, MW. 2013. Strong latitudinal patterns in the elemental ratios of marine plankton and organic matter. *Nature Geoscience* **6**(4): 279–283. DOI: https://dx.doi.org/10.1038/ngeo1757.

Meiners, KM, Brinkmeyer, R, Granskog, MA, Lindfors, A. 2004. Abundance, size distribution and bacterial colonization of exopolymer particles in Antarctic sea ice (Bellingshausen Sea). *Aquatic Microbial Ecology* **35**: 283–296. DOI: https://dx.doi.org/10.3354/ame035283.

Meiners, KM, Gradinger, R, Fehling, J, Civitarese, G, Spindler, M. 2003. Vertical distribution of exopolymer particles in sea ice of the Fram Strait (Arctic) during autumn. *Marine Ecology Progress Series* **248**: 1–13. DOI: https://dx.doi.org/10.3354/meps248001.

Meiners, KM, Krembs, C, Gradinger, R. 2008. Exopolymer particles: Microbial hotspots of enhanced bacterial activity in Arctic fast ice (Chukchi Sea). *Aquatic Microbial Ecology* **52**(2): 195–207. DOI: https://dx.doi.org/10.3354/ame01214.

Meiners, KM, Vancoppenolle, M, Carnat, G, Castellani, G, Delille, B, Delille, D, Dieckmann, GS, Flores, H, Fripiat, F, Grotti, M, Lange, BA, Lannuzel, D, Martin, A, McMinn, A, Nomura, D, Peeken, I, Rivaro, P, Ryan, KG, Stefels, J, Swadling, KM, Thomas, DN, Tison, J-L, van der Merwe, P, van Leeuwe, MA, Weldrick, C, Yang, EJ. 2018. Chlorophyll-a in Antarctic landfast sea ice: A first synthesis of historical ice core data. *Journal of Geophysical Research: Ocean* **123**(11): 8444–8459. DOI: https://dx.doi.org/10.1029/2018JC014245.

Miller, LA, Fripiat, F, Else, BGTT, Bowman, JS, Brown, KA, Collins, RE, Ewert, M, Fransson, A, Gosselin, M, Lannuzel, D, Meiners, KM, Michel, C, Nishioka, J, Nomura, D, Papadimitriou, S, Russell, LM, Sørensen, LL, Thomas, DN, Tison, J-L, van Leeuwe, MA, Vancoppenolle, M, Wolff, EW, Zhou, J. 2015. Methods for biogeochemical studies of sea ice: The state of the art, caveats, and recommendations. *Elementa: Science of the Anthropocene* **3**: 38. DOI: https://dx.doi.org/10.12952/journal.elementa.000038.

Mundy, CJ, Barber, DG, Michel, C. 2005. Variability of snow and ice thermal, physical and optical properties pertinent to sea ice algae biomass during spring. *Journal of Marine Systems* **58**(3–4): 107–120. DOI: https://dx.doi.org/10.1016/j.jmarsys.2005.07.003.

Ragueneau, O, Savoye, N, Del Amo, Y, Cotten, J, Tardiveau, B, Leynaert, A. 2005. A new method for the measurement of biogenic silica in suspended matter of coastal waters: Using Si:Al ratios to correct for the mineral interference. *Continental Shelf Research* **25**: 697–710. DOI: https://dx.doi.org/10.1016/j.csr.2004.09.017.

Riaux-Gobin, C, Dieckmann, GS, Poulin, M, Neveux, J, Labrune, C, Vétion, G. 2013. Environmental conditions, particle flux and sympagic microalgal succession in spring before the sea-ice break-up in Adélie Land, East Antarctica. *Polar Research* **32**(Suppl.): 0–25. DOI: https://dx.doi.org/10.3402/polar.v32i0.19675.

Riaux-Gobin, C, Tréguer, P, Dieckmann, GS, Maria, E, Vétion, G, Poulin, M. 2005. Land-fast ice off Adélie Land (Antarctica): Short-term variations in nutrients and chlorophyll just before ice break-up. *Journal of Marine Systems* **55**(3–4): 235–248. DOI: https://dx.doi.org/10.1016/j.jmarsys.2004.08.003.

Riedel, A, Michel, C, Gosselin, M, LeBlanc, B. 2007. Enrichment of nutrients, exopolymeric substances and microorganisms in newly formed sea ice on the Mackenzie shelf. *Marine Ecology Progress Series* **342**: 55–67.

Roukaerts, A, Cavagna, A-J, Fripiat, F, Lannuzel, D, Meiners, KM, Dehairs, F. 2016. Sea-ice algal primary production and nitrogen uptake rates off East Antarctica. *Deep Sea Research Part II: Topical Studies in Oceanography* **131**: 140–149. DOI: https://dx.doi.org/10.1016/j.dsr2.2015.08.007.

Rysgaard, S, Glud, RN, Sejr, MK, Blicher, ME, Stahl, HJ. 2008. Denitrification activity and oxygen dynamics in Arctic sea ice. *Polar Biology* **31**(5): 527–537. DOI: https://dx.doi.org/10.1007/s00300-007-0384-x.

Smith, REH, Harrison, WG, Harris, LR, Herman, AW. 1990. Vertical fine structure of particulate matter and nutrients in sea ice of the High Arctic. *Canadian Journal of Fisheries and Aquatic Sciences* **47**: 1348–1355. DOI: https://dx.doi.org/10.1139/f90-154.

Stewart, PS, Franklin, MJ. 2008. Physiological heterogeneity in biofilms. *Nature Reviews Microbiology* **6**(3): 199–210. DOI: https://dx.doi.org/10.1038/nrmicro1838.

Thomas, DN, Dieckmann, GS. 2002. Biogeochemistry of Antarctic sea ice. *Oceanography and Marine Biology* **40**: 143–170.

Tison, JL, Lorrain, RD, Bouzette, A, Dini, M, Bondesan, A, Stievenard, M. 1998. Linking landfast sea ice variability to marine ice accretion at Hells Gate Ice Shelf, Ross Sea, in Jeffries, MO ed., *Antarctic sea ice: Physical processes, interactions and variability* (Antarctic research series; vol. 74). Washington, DC: American Geophysical Union: 375–407.

Underwood, GJC, Fietz, S, Papadimitriou, S, Thomas, DN, Dieckmann, GS. 2010. Distribution and composition of dissolved extracellular polymeric substances (EPS) in Antarctic sea ice. *Marine Ecology Progress Series* **404**: 1–19. DOI: https://dx.doi.org/10.3354/meps08557.

Vancoppenolle, M, Meiners, KM, Michel, C, Bopp, L, Brabant, F, Carnat, G, Delille, B, Lannuzel, D, Madec, G, Moreau, S, Tison, J-L, van der Merwe,

P. 2013. Role of sea ice in global biogeochemical cycles: Emerging views and challenges. *Quaternary Science Reviews* **79**: 207–230. DOI: https://dx.doi.org/10.1016/j.quascirev.2013.04.011.

Vancoppenolle, M, Tedesco, L. 2017. Numerical models of sea ice biogeochemistry, in Thomas, DN ed., *Sea ice*. Third edition. Hoboken, NJ: Wiley & Sons: 492–515. DOI: https://dx.doi.org/10.1002/9781118778371.ch20.

Van der Linden, FC, Tison, J-LL, Champenois, W, Moreau, S, Carnat, G, Kotovitch, M, Fripiat, F, Deman, F, Roukaerts, A, Dehairs, F, Wauthy, S, Lourenço, A, Vivier, F, Haskell, T, Delille, B. 2020. Sea ice CO2 dynamics across seasons: Impact of processes at the interfaces. *Journal of Geophysical Research: Oceans* **125**. DOI: https://dx.doi.org/10.1029/2019JC015807.

van der Merwe, P, Lannuzel, D, Bowie, AR, Meiners, KM. 2011. High temporal resolution observations of spring fast ice melt and seawater iron enrichment in East Antarctica. *Journal of Geophysical Research: Biogeosciences* **116**(3): 1–18. DOI: https://dx.doi.org/10.1029/2010JG001628.

Vert, M, Doi, Y, Hellwich, K-H, Hess, M, Hodge, P, Kubisa, P, Rinaudo, M, Schué, F. 2012. Terminology for biorelated polymers and applications (IUPAC Recommendations 2012). *Pure and Applied Chemistry* **84**(2): 377–410. DOI: https://dx.doi.org/10.1351/PAC-REC-10-12-04.

Zhang, JZ, Ortner, PB. 1998. Effect of thawing condition on the recovery of reactive silicic acid from frozen natural water samples. *Water Research* **32**(8): 2553–2555. DOI: https://dx.doi.org/10.1016/S0043-1354(98)00005-0.

How to cite this article: Roukaerts, A, Deman, F, Linden, FVD, Carnat, G, Bratkic, A, Moreau, S, Lannuzel, D, Dehairs, F, Delille, B, Tison, J-L, Fripiat, F. 2021. The biogeochemical role of a microbial biofilm in sea ice: Antarctic landfast sea ice as a case study. *Elementa: Science of the Anthropocene* 9(1). DOI: https://doi.org/10.1525/elementa.2020.00134

Domain Editor-in-Chief: Jody W. Deming, University of Washington, Seattle, WA, USA

Associate Editor: Christine Michel, Department of Fisheries and Oceans, Canada

Knowledge Domain: Ocean Science and Ecology & Earth Systems

Published: June 14, 2021 **Accepted:** May 13, 2021 **Submitted:** September 8, 2020

ELEMENTA Science of the Anthropocene

Elem Sci Anth is a peer-reviewed open access journal published by University of California Press.

OPEN ACCESS